THE JOURNAL OF COMPARATIVE NEUROLOGY 457:185–201 (2003)

Inner S-Cone Bipolar Cells Provide All of the Central Elements for S Cones in Macaque Retina

STEVE HERR,[1] KARL KLUG,[2] PETER STERLING,[3] AND STAN SCHEIN[1,2]*
[1]Department of Psychology, Franz Hall, University of California, Los Angeles, Los Angeles, California 90095-1563
[2]Brain Research Institute, University of California, Los Angeles, Los Angeles, California 90095-1761
[3]Department of Neuroscience, University of Pennsylvania, Philadelphia, Pennsylvania 19104

ABSTRACT

Synaptic terminals of cones (*pedicles*) are presynaptic to numerous processes that arise from the dendrites of many types of bipolar cell. One kind of process, a *central element,* reaches deeply into invaginations of the cone pedicle just below an active zone associated with a synaptic ribbon. By reconstruction from serial electron micrographs, we show that L- and M-cone pedicles in macaque fovea are presynaptic to ~20 central elements that arise from two types of *inner* (invaginating) bipolar cell, midget and diffuse. In contrast, S-cone pedicles, with more synaptic ribbons, active zones/ribbon, and central elements/active zone, are presynaptic to ~33 central elements. Moreover, all of these arise from *one* type of bipolar cell, previously described by others, here termed an *inner S-cone bipolar cell.* Each provides ~16 central elements. Thirty-three is twice 16; correspondingly, these bipolar cells are twice as numerous as S cones. (Specifically, each S cone is presynaptic to four inner S-cone bipolar cells; in turn, each bipolar cell provides central elements to two S cones.) These bipolar cells are presynaptic to an equal number of small-field bistratified ganglion cells, giving cell numbers in 2G:2B:1S ratios. Each ganglion cell receives input from two or more inner S-cone bipolar cells and thereby collects signals from three or more S cones. This convergence, along with chromatic aberration of short-wavelength light, suggests that S-cone contributions to this ganglion cell's coextensive *blue-ON/yellow-OFF* receptive field are larger than opponent L/M-cone contributions via outer diffuse bipolar cells and that opponent L/M-cone signals are conveyed mainly by inner S-cone bipolar cells. J. Comp. Neurol. 457:185–201, 2003.

Indexing terms: photoreceptors (vertebrate); presynaptic terminals; synapses; synaptic membranes; color perception; retinal ganglion cells

The synaptic terminals (*pedicles*) of all three cone types (L, M, and S) in the fovea of macaque monkey contain ~20 synaptic ribbons (Esfahani et al., 1993; Calkins et al., 1996). In cross-sectional view, such as that shown in Figure 1A, each ribbon appears to be presynaptic to a *triad* of invaginating elements (Sjöstrand, 1958; Missotten, 1962, 1965): two lateral elements provided by horizontal cell dendrites (Stell, 1967) and one central element provided by an *invaginating* bipolar cell dendrite (Dowling and Boycott, 1966; Boycott and Dowling, 1969). [In fact, *several* central elements may line up in single file beneath a ribbon (Chun et al., 1996; Migdale et al., 2003; see also below).] Invaginating bipolar cells have their syn-

Grant sponsor: National Institute of Mental Health; Grant number: MH15795-18; Grant sponsor: National Institute of Health; Grant number: EY11153; Grant number: EY08124.

*Correspondence to: Stan Schein, Department of Psychology, Franz Hall, Mail Code 951563, University of California, Los Angeles, Los Angeles, CA 90095-1563. E-mail: schein@ucla.edu

Received 6 June 2002; Revised 24 September 2002; Accepted 31 October 2002

DOI 10.1002/cne.10553

Published online the week of January 20, 2003 in Wiley InterScience (www.interscience.wiley.com).

aptic terminals in the inner half of the inner plexiform layer (IPL), where they make excitatory synapses with physiologically ON-center ganglion cells (Famiglietti and Kolb, 1976; Nelson et al., 1978). Following Dacey (1993a), we refer to these as *inner* bipolar cells.

L- and M-cone pedicles are presynaptic to two types of inner bipolar cell, midget and diffuse, both of which contribute multiple central elements (Kolb, 1970; Hopkins and Boycott, 1995; Calkins et al., 1996; Chun et al., 1996). The midget bipolar cell is commonly regarded as cone-type specific, because, in the fovea at least, it is postsynaptic to a single cone (Polyak, 1941) and thus necessarily a single *type* of cone.

S-cone pedicles are presynaptic to a special kind of *inner S-cone bipolar cell,* whose dendrites are contacted only by S-cone pedicles—usually several of them, in contrast to the case for foveal midget bipolar cells—and whose terminals are located in the innermost sublayer of the inner (ON) half of the IPL (Mariani, 1984; Kouyama and Marshak, 1992; Wässle et al., 1994). [The authors cited called these cells *blue-cone bipolar cells.* Each S cone, however, is also presynaptic to an outer (OFF) midget bipolar cell (Klug et al., 1992; see also Valberg et al., 1986), necessarily S-cone specific, so the term *blue-cone bipolar cell* must be qualified with *inner.*] Inner S-cone bipolar cells synapse onto a distinct type of ganglion cell, a small-field (or simply *small*), bistratified one (Rodieck, 1991; Dacey, 1993b; Calkins et al., 1998). True to its name, this ganglion cell has a second set of dendrites that ramifies in the outer (OFF) half of the IPL, where they are postsynaptic to outer diffuse bipolar cells.

Electrophysiological recordings of these ganglion cells show that they are excited by short-wavelength (blue) light and inhibited by middle- and long-wavelength light (Dacey and Lee, 1994). The chromatically antagonistic response of this blue-ON/yellow-OFF ganglion (and lateral geniculate nucleus) cell (Wiesel and Hubel, 1966; de Monasterio and Gouras, 1975; Derrington et al., 1984; Lennie and D'Zmura, 1988) suggests that it is the neural correlate of the perceptual blueness-yellowness color opponent pair (Dacey and Lee, 1994; Calkins et al., 1998; Cottaris and DeValois, 1998; Dacey, 2000).

An S cone contacts no inner *midget* bipolar cell (Klug et al., 1991), so it may be supposed that the special inner S-cone bipolar cell takes its place. We explored this supposition by asking if the number of central elements provided by inner S-cone bipolar cells to S cones were similar to the number of central elements provided by inner midget bipolar cells to L and M cones.

By using an anti-CCK antibody that selectively labels inner S-cone bipolar cells, Kouyama and Marshak (1992) labeled only some (e.g., 8 of 30) of the central elements postsynaptic to an S cone, suggesting that another type of bipolar cell, specifically an inner diffuse one, provided the remaining central elements. Therefore, from serial electron micrographs, we tracked and characterized the bipolar cells responsible for the central elements of every triad in several S-cone pedicles.

Against expectation, we found that *every* S-cone central element is provided by just *one* type of bipolar cell, the inner S-cone bipolar cell. We also found that many synaptic ribbons in S cones are presynaptic to multiple central elements, which are generally provided by different inner S-cone bipolar cells. In light of the understaining by Kouyama and Marshak (1992), suspected by the authors themselves and affirmed by Wässle et al. (1994) and now by us, we reinvestigated the overall pattern of divergence and convergence of S cones with inner S-cone bipolar cells. Portions of this work were presented earlier in abstract form (Herr et al., 1996).

MATERIALS AND METHODS

A retina was removed from an adult (6 kg), male (*Macaca fascicularis*) monkey that had been anesthetized (40 mg/kg pentobarbital) and perfused with a phosphate-buffered (pH 7.4) solution of 2% glutaraldehyde and 2% paraformaldehyde in accordance with Assurance Number A3332-01 from the Institutional Animal Care and Use Committee of the Massachusetts Eye and Ear Infirmary. The retina was postfixed by immersion in 2% OsO_4 in 8% dextrose for 30 minutes at 4°C and 60 minutes at 22°C. A strip of retina containing the fovea was then dissected, stained *en bloc* in 1% aqueous uranyl acetate, dehydrated, and embedded in Epon. A series of 319 ultrathin (90 nm), vertical sections was cut parallel to the horizontal meridian, through the foveal center. These serial cross sections were mounted on formvar-coated slot grids and stained with uranyl acetate and lead citrate. The region from 460 to 640 μm nasal to the foveal center was photographed *en montage* at 2,000× and 5,000× in an electron microscope (Tsukamoto et al., 1992). Four complete and one incomplete S-cone pedicles and eight L- and M-cone pedicles, were rephotographed at 10,000× (Fig. 1A). Negatives were printed at 2.5× or 3.5× enlargement. Electron photomicrographs in the figures, photographed at 10,000× and printed at 25,000×, were scanned with an Agfa scanner. Aside from linear adjustment for brightness and contrast, no retouching or other image manipulation was performed. Because of lateral displacement of photoreceptor terminals from cone inner segments (Schein, 1988), the center of the photographed region corresponded to ~1° of eccentricity in the visual field (Calkins et al., 1994). The macaque fovea has a radius of 500 μm, or 2.5°, so the photoreceptors that contacted this region were well within the fovea (Polyak, 1941).

The six S-cone pedicles in our series (Fig. 2) were identified in several ways (Klug et al., 1991; Herr et al., 1996). First, the S-cone pedicles were smaller in volume than the L- and M-cone pedicles (Esfahani et al., 1993), consistently with the findings of Ahnelt et al. (1990). Second, the number of synaptic ribbons in each S-cone pedicle was greater than 20, whereas we observed 20 or fewer ribbons in the other cone pedicles (Esfahani et al., 1993; Calkins et al., 1996). Third, the S-cone pedicles contacted only one type of midget bipolar cell, an outer type, but the L- and M-cone pedicles contacted both inner and outer midget bipolar cells (Klug et al., 1992). Fourth, the S-cone pedicles in our series contacted a special type of bipolar cell, the inner S-cone bipolar cell, which itself is generally contacted by multiple S-cone pedicles but not intervening cone pedicles (Mariani, 1984; Kouyama and Marshak, 1992; Wässle et al., 1994). Fifth, in cases in which the axon terminals of inner S-cone bipolar cells in our series could be tracked, these terminals were observed to contact small bistratified ganglion cells in the inner (ON) stratum of the IPL (Calkins et al., 1998). We observed additional differences that are reported below.

From the series of electron micrographs, we tracked the dendritic branch responsible for each central element in-

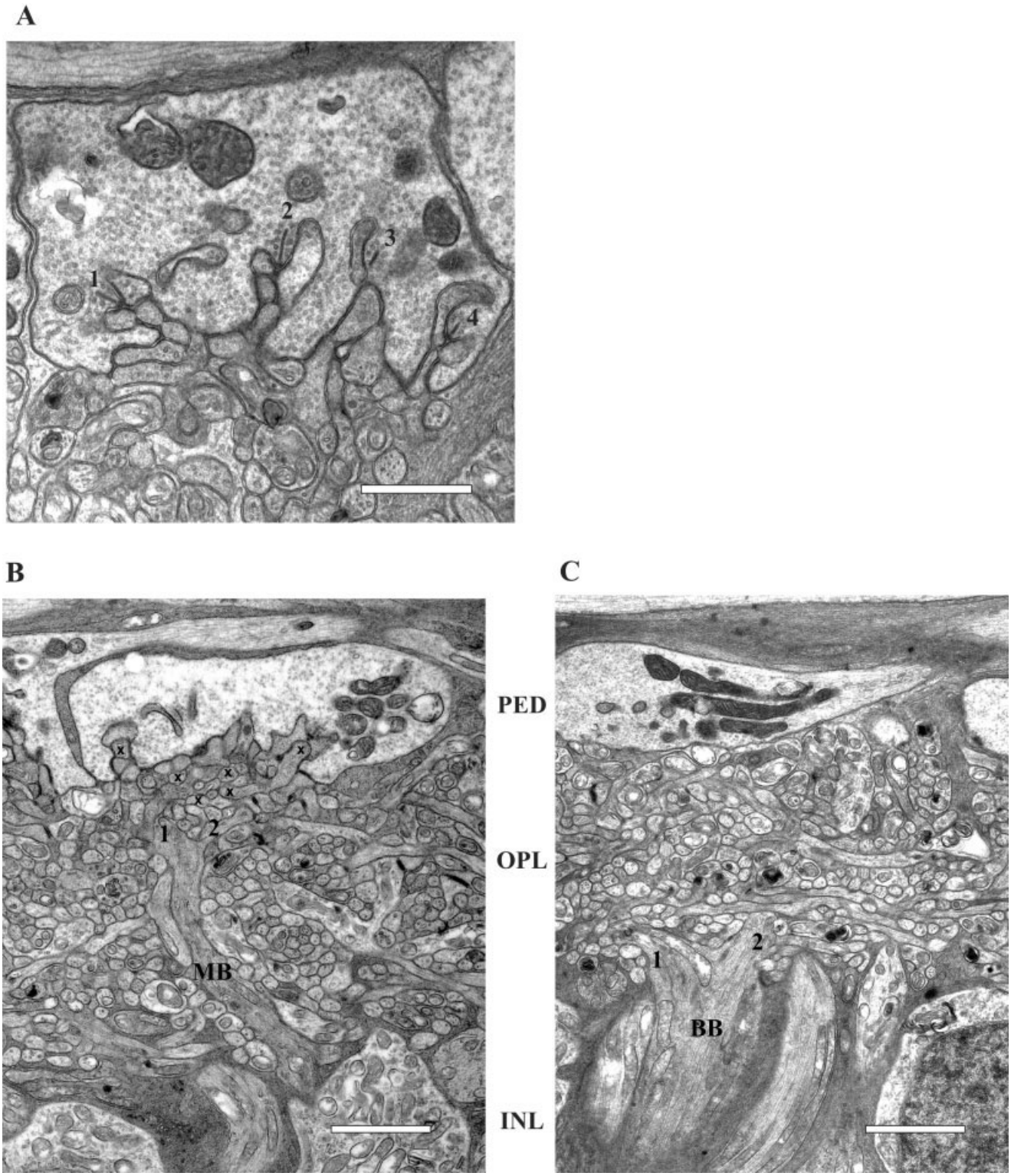

Fig. 1. Cross sections of the outer plexiform layer (OPL). **A:** S-cone pedicle No. 76, showing four synaptic ribbons. Each ribbon is presynaptic to a triad of postsynaptic elements, the central element provided by an inner (invaginating or ON) bipolar cell dendrite. These particular four ribbons are presynaptic to nine central elements in all. **B:** The main dendrite of an inner midget bipolar cell (MB), contacted by an L or M cone, branches close to its cone pedicle, in the *outer* part of the OPL, to form a bouquet of large branches (1 and 2) and finer branches (x). **C:** The main dendrite of an inner S-cone bipolar cell splits into primary branches (1 and 2) in the *innermost* stratum of the OPL. Scale bars = 1 μm.

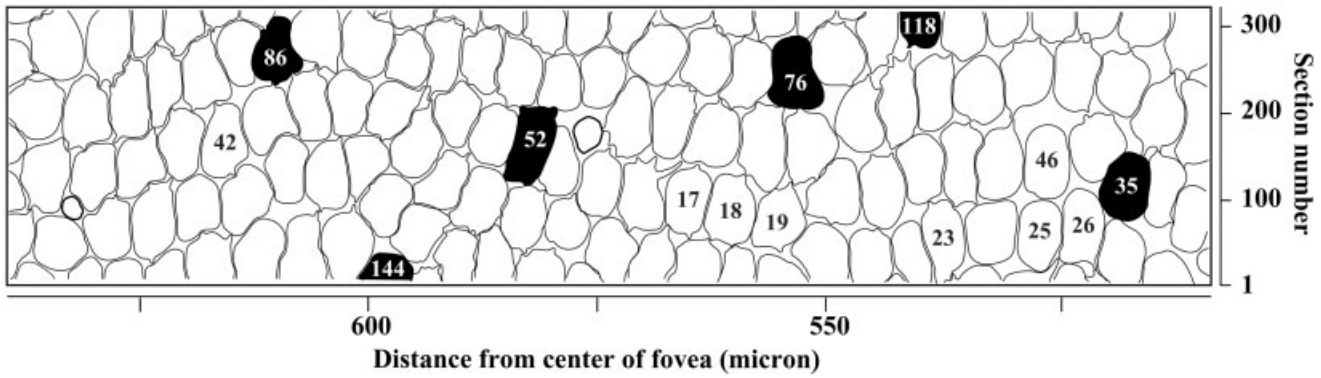

Fig. 2. Map of the cone pedicles in the series with four complete S cones and two incomplete S cones (solid areas with white numbers) along with eight L and M cones (open areas with black numbers). The two terminals with thicker contours are rod spherules. This map, modified from Tsukamoto et al. (1992), corresponds to a hypothetical tangential section through the layer of cone pedicles and was created by reconstruction from 319 serial cross sections.

ward to its main dendrite and then outward through the bipolar cell's entire dendritic tree. Where possible, we also tracked the dendrite to the cell's soma and axon terminal. We tracked all of the central elements in the four complete and two incomplete S-cone pedicles in our series. For comparison, we identified the nature of the bipolar cell providing each central element in eight L and M cones (Fig. 2). The dendritic branches and their invaginating contacts were traced by hand onto clear plastic sheets. To create a three-dimensional (3D) data set, the superimposed tracings were aligned and digitized into a computer running Montage software (Smith, 1987). The same procedure (tracing, alignment, digitization) was utilized to reconstruct a *hybrid* surface of the S-cone pedicle along with its synaptic ribbons.

We tiled the 3D data sets with Ken Sloan's Contour Fitter program (Meyers, 1992). We produced the visualizations in Figures 6–9 with the Geomview package from the Geometry Center, University of Minnesota (http://www.geom.umn.edu/software/geomview/) and the surfaces in Figures 7 and 9B with Blue Moon Rendering Tools (http://www.bmrt.org).

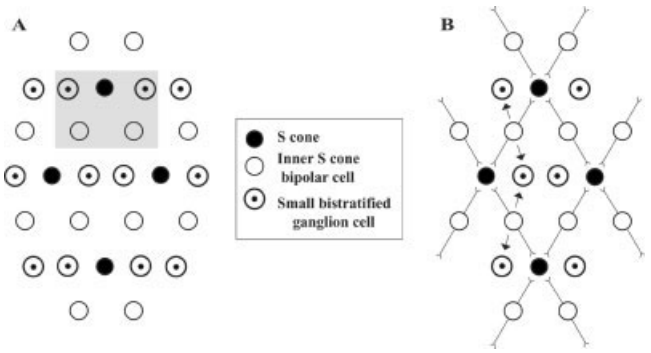

Fig. 3. Diagrams showing relative numbers and connections among S cones, inner S-cone bipolar cells, and small bistratified ganglion cells. **A:** For each S cone, this pattern has two inner S-cone bipolar cells and two small bistratified ganglion cells. The gray box merely serves to assist in seeing the 1S:2B:2G ratio. **B:** Each S cone is presynaptic to the central processes of four inner S-cone bipolar cells; in turn, each inner S-cone bipolar cell provides central processes to two S cones. Each inner S-cone bipolar cell is presynaptic to two small bistratified ganglion cells; in turn, each small bistratified ganglion cell collects input from two inner S-cone bipolar cells. In this arrangement, each small bistratified ganglion cell collects signals from three S cones.

RESULTS

Figure 3 summarizes a large body of the results that are presented here: The ratios of numbers of small bistratified ganglion cells, inner S-cone bipolar cells, and S cones are 2:2:1 in macaque fovea (Fig. 3A). Each S cone is presynaptic to four inner S-cone bipolar cells; in turn, each inner S-cone bipolar cell provides central elements to two S cones (Fig. 3B). Each inner S-cone bipolar cell is presynaptic to two small bistratified ganglion cells; in turn, each small bistratified ganglion cell is postsynaptic to two inner S-cone bipolar cells (Fig. 3B). Thus, foveal small bistratified ganglion cells collect signals from at least three S cones.

S cones are presynaptic to more central elements than L and M cones

We studied four complete and two incomplete S-cone pedicles. Each complete S-cone pedicle had 21–23 ribbons; the incomplete ones had 19 and 10 (Table 1A). By comparison, the L and M cones had 17–20 ribbons (Table 1B). In cross section (Fig. 1A), each ribbon contacted a triad of invaginating elements: two lateral elements provided by horizontal cell dendrites and a central element provided by an inner bipolar cell dendrite (Missotten, 1965; Dowling and Boycott, 1966; Stell, 1967). An arciform density lay along the base of the ribbon and marked the active zone, the region where synaptic vesicles fuse and release glutamate. Most ribbons had one active zone and one pair of apposed lateral elements.

Some S-cone ribbons had two active zones. The two halves L1 and L2 of the ribbon shown on the left in Figure 4 were separated by a short *gap,* where the ribbon pulled away from the presynaptic membrane and was missing its arciform density (see particularly Fig. 4B,C). Each half had its own pair of lateral elements. Perhaps as a consequence of maintaining two active zones, these *double ribbons* were generally longer than average. We found one or

TABLE 1A. Number of Each Type of Active Zone in S-Cone Synaptic Ribbons

Pedicle no.	No.of ribbons	Double ribbons[1]	Active zones	Singlet[2]	Doublet[2]	Triplet[2]	Quad[2]	Multiplet active zones[3]	Shared central elements[4]	No. of central elements[5]	Central elements in multiplets[6]	Multiplets showing exclusivity[7]
35	22	2	24	16	6 (6)	2 (1)	0	8 (33%)	3	31	18 (58%)	7/8
52	23	2	25	9	9 (9)	6 (4)*	1 (0)*	16 (64%)	6	43	38 (88%)	13/16
76	21	2	23	11	10 (8)*	2 (1)	0	12 (52%)	5	31†	23 (74%)	9/12
86	23	1	24	16	7 (6)	1 (1)	0	8 (33%)	5	28	16 (57%)	7/8
118[8]	19[8]	0[8]	19[8]	11[8]	7 (6)[8]	1 (1)[8]	0[8]	8[8]	5[8]	21[8]†	9 (32%)	7/8
144[8]	10[8]	0[8]	10[8]	2[8]	7[8]	1[8]	0[8]	8[8]	2[8]	17[8]	15 (88%)[8]	
Total	118	7	125	65	46	13	1	60 (48%)	26	171	119 (70%)	35/52 (83%)

[1]A *double ribbon* has two active zones, each with its own pair of lateral processes.
[2]A *singlet* active zone has one central element, a *doublet* has two, a *triplet* has three, and a *quad* has four. The number in parentheses refers to the number of doublets, triplets, etc., all of whose central elements are provided by different inner S-cone bipolar cells. In cases marked by an asterisk (*), one of the two, three, or four central elements from the same inner S-cone bipolar cell was shared with another active zone.
[3]A *multiplet active zone* is any active zone with more than one central element, e.g., a triplet.
[4]*Shared central elements* serve two or even three active zones.
[5]The total *number of central elements* is equal to the sum from the (singlet = 1, doublet = 2, etc.) data minus the number of shared central elements. In pedicle #76, however, one central element was shared by three active zones, so the total number (†) was one less than that calculation, and, in pedicle #118, two central elements were shared by three active zones, so the total number (†) was two less than that calculation.
[6]The number of *central elements in multiplets* is accompanied by its percentage of all the central elements in parentheses.
[7]The numbers of *multiplets showing exclusivity* are those doublets, triplets, etc., all of whose central elements are provided by different inner S-cone bipolar cells. This number is equal to the sum of the numbers in parentheses in the doublet, triplet, and quad columns.
[8]This pedicle was not complete, or this number characterizes an incomplete pedicle.

TABLE 1B. Number of Each Type of Active Zone in Synaptic Ribbons of L and M Cones

Pedicle no.	No. of ribbons	Double ribbons[1]	Active zones	Singlet[2]	Doublet[2]	Triplet[2]	Multiplet active zones[3]	Shared central elements[4]	No. of central elements[5]	Central elements in multiplets[6]	Multiplet types[7]			Multiplets showing exclusivity[8]
											MM	MD	DD	
17	19	0	19	16	3	0	3 (16%)	2	19†	6 (32%)	1	2	0	2/3
18	19	0	19	16	3	0	3 (16%)	4	18	6 (33%)	0	2	1	3/3
19	19	0	19	14	5	0	5 (26%)	4	20	10 (50%)	3	2	0	2/5
23	20	0	20	15	5	0	5 (25%)	2	23	10 (43%)	2	2	1	3/5
25	17	0	17	10	6	1	7 (41%)	1	24	15 (63%)	0	7	0	7/7
26	19	0	19	19	0	0	0 (0%)	2	17	0 (0%)	0	0	0	0/0
42	17	0	17	16	1	0	1 (6%)	1	17	2 (12%)	0	1	0	1/1
46	19	0	19	17	2	0	2 (11%)	2	19	4 (21%)	1	1	0	1/2
Total	149	0	149	123	25	1	26 (17%)	18	157	53 (34%)	7	17	2	19/26 (73%)

[1]A *double ribbon* has two active zones, each with its own pair of lateral processes.
[2]A *singlet* active zone has one central element, a *doublet* has two, a *triplet* has three, and a *quad* has four.
[3]A *multiplet active zone* is any active zone with more than one central element, e.g., a triplet.
[4]*Shared central elements* serve two or even three active zones.
[5]The total *number of central elements* is equal to the sum from the (singlet = 1, doublet = 2, etc.) data minus the number of shared central elements. In pedicle #17, however, one central element was shared by three active zones, so the total number (†) was one less than that calculation.
[6]The number of *central elements in multiplets* is accompanied by its percentage of all the central elements in parentheses.
[7]Central elements in multiplet active zones may be provided by a single midget bipolar cell only (MM), one midget and one diffuse bipolar cell (MD), or one or two different diffuse bipolar cells (DD).
[8]The number of *multiplets showing exclusivity* counts those multiplets, all of whose central elements are provided by different bipolar cells. This number is equal to the number in the MD column and some from the DD column.

two of these double ribbons (with two active zones each) in every one of the four complete S cones in our series (Table 1A). Because the double ribbons had two active zones, the total number of active zones (or ribbon synaptic units) in each S-cone pedicle was 23–25 (Table 1A). By contrast, we found only one double ribbon in 19 L- and M-cone pedicles, so the number of active zones in L and M cones was nearly always equal to the number of ribbons (Table 1B) and lower (17–20) than that found in S cones.

Many active zones in all cone types were presynaptic to several central elements, even though they may appear in a single section to be presynaptic to just one. For example, in Figure 1A, color coded in Figure 5, the dendrite below the central element of triad 2 takes a central position a few sections away, and these particular four ribbons are presynaptic to nine central elements in all. The sequence of micrographs from an S-cone pedicle shown in Figure 4 shows four central elements (3, 4, 7, and 8) associated with the ribbon/active zone R. In color Figure 6, the three-dimensional reconstruction of ribbon R with three of its four central elements and one (L2) active zone of the double ribbon to its left shows that the central elements were lined up in single file along the length of the bottom of the ribbon. Without the aid of reconstruction, because of plane of section, Figures 3D and 3E show that the L1 active zone of the double ribbon was presynaptic to a series of three central elements (1, 5, and 6) that can be seen to line up in single file as well. The single file arrangement held for all active zones that were presynaptic to several central elements.

Some central elements were shared by two active zones. The right active zone (L2) of the double ribbon shown in Figure 4 was also presynaptic to a series of three central elements (2, 6, and 7). The L1 and L2 active zones of the double ribbon on the left shared central element 6, as can be seen clearly in Figure 4D. Sharing of a central element occurred between two synaptic ribbons as well; for example, central element 7 was shared between ribbon R on the right (Fig. 4E) and the L2 active zone of the double ribbon on the left (Fig. 4D). Sharing of central element 7 can also be seen in stereo color Figure 6. Each complete S-cone pedicle had three to six central elements that were shared by two active zones (Table 1A). In a horizontal plane of section, the two pairs of lateral elements of the two rib-

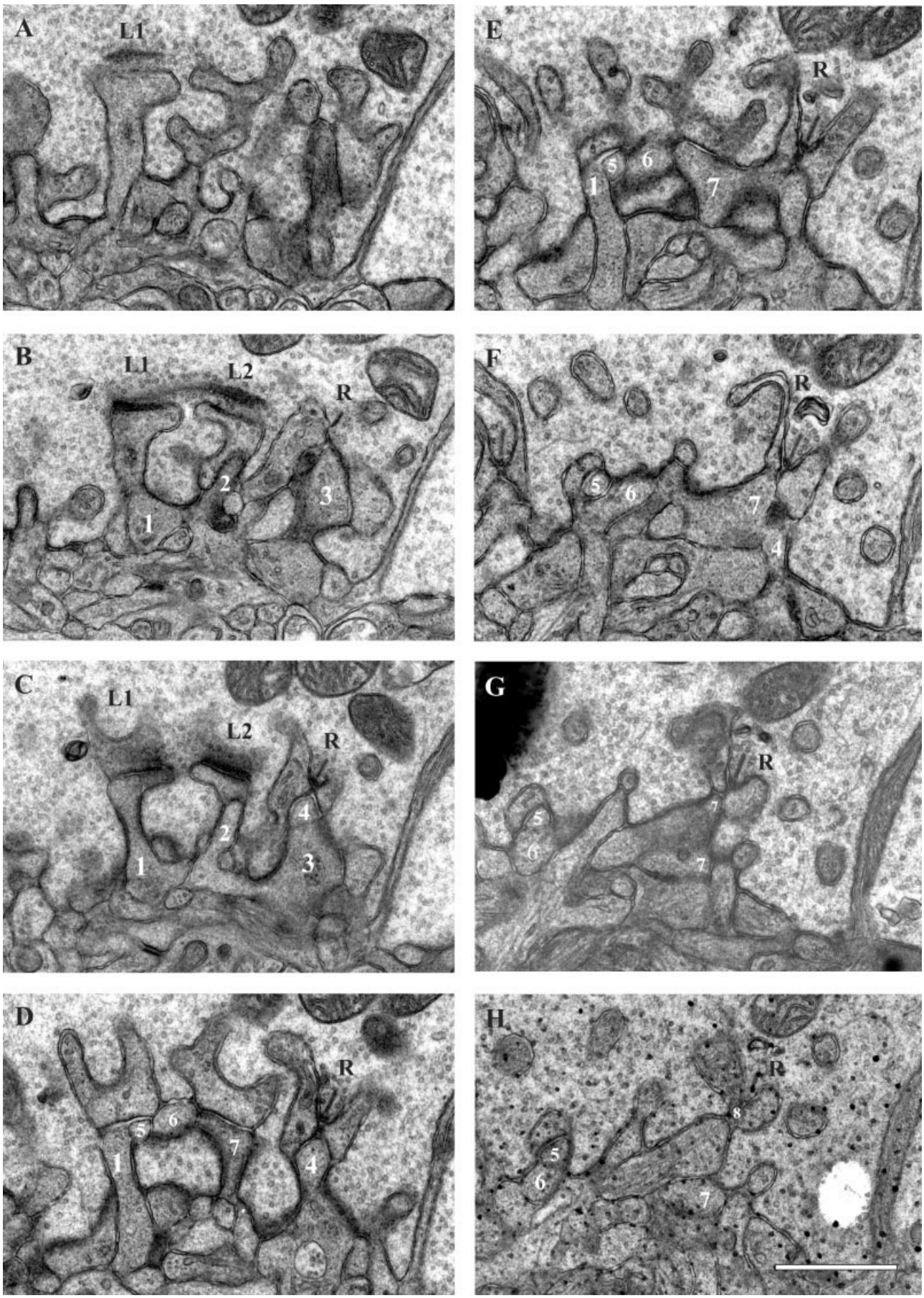
A
L1
E
R
1
5
6
7
B
L1
L2
R
2
3
1
F
R
5
6
7
4
C
L1
L2
R
4
2
1
3
G
R
5
6
7
7
D
R
5
6
1
7
4
H
R
8
5
6
7

Figure 4

bons (or the two pairs of lateral elements of a double ribbon) and their shared central element could have a *butterfly* appearance, as in Figure 4D, similar to that shown by Chun et al. (1996). Shared central elements were somewhat less common in L and M cones (Table 1B).

We categorized active zones by the number of central elements to which they were presynaptic. We called an active zone that was presynaptic to one central element a *singlet,* an active zone that was presynaptic to two central elements a *doublet,* and so on. We studied 125 active zones in the six S-cone pedicles in our series, and 60 (48%) were presynaptic to multiple central elements (Table 1A). By contrast, only 26 (17%) of the 149 active zones in the eight L- and M-cone pedicles that we studied were presynaptic to more than one central element (Table 1B).

The number of singlet active zones, plus two times the number of doublet active zones, plus three times the number of triplet active zones, and so on, minus the number of central elements shared by two active zones, gives the total number of central elements (Table 1A,B). A large percentage of the central elements was found in *multiplet* active zones, our name for active zones with more than one central element, from 57% to 88% in our sample of S cones, averaging 73% over the four complete S cones. Fewer central elements of L and M cones were found in multiplet active zones, from 0% to 63%, averaging 34%. Because S cones had more ribbons than L and M cones, because more ribbons in S cones had more than one active zone, and because active zones in S cones were more likely to have multiple central elements, the number of central elements postsynaptic to S cones, 28–43 (mean 33.3), was substantially greater than the number of central elements postsynaptic to L and M cones, 17–24 (mean 19.6).

Inner S-cone bipolar cells are distinct from inner midget bipolar cells

After tracking the central elements postsynaptic to the S-cone pedicles in our series to their main dendrites, we tracked the entire dendritic trees of these bipolar cells back to the pedicle layer. We identified several inner S-cone bipolar *cells* that had their main dendrite and soma within our series, one that had its main dendrite but not its soma within the series, and several additional inner S-cone bipolar cell *dendrites* that were missing main dendrites and cell bodies. The evidence that these were inner S-cone bipolar cells or dendrites followed Mariani (1984), Kouyama and Marshak (1992), and Wässle et al. (1994), is summarized in Table 2, and is described below.

The main dendrite of an inner midget bipolar cell splits close to its L- or M-cone pedicle (Fig. 1B), in the outer region of the outer plexiform layer (OPL). By contrast, each inner S-cone bipolar cell projects a single *main dendrite* through the inner nuclear layer, which then splits as it reaches the innermost region of the OPL (Fig. 1C), ultimately supplying an average of six *primary branches.* For example, one inner S-cone bipolar cell, iSB2, contributed five primary branches to S-cone pedicle #52 (color Fig. 7) as well as two other primary branches to other S-cone pedicles.

Each inner S-cone bipolar cell's primary branch reached just one S-cone pedicle as a *"bundle" of fine dendritic branches,* ultimately supplying several *central elements.* For example, the five primary branches shown in Figure 7 contributed five, two, two, one, and one central elements to S-cone pedicle #52. [In addition, every one of our inner S-cone bipolar cells had several fine dendritic branches that definitively failed to reach any S-cone pedicle but ended instead in the OPL as *blind dendrites,* as previously described by Mariani (1984) for inner S-cone bipolar cells and questioned by Wässle et al. (1994).] As can be appreciated by a comparison of the map of pedicles in Figure 2 with the reconstruction of inner S-cone bipolar cells shown in Figure 8, each primary branch skipped the non-S-cone pedicles in its neighborhood on the way to an S-cone pedicle. Only one inner S-cone bipolar cell, iSB5, had all of its primary branches converge onto a single S cone.

Four inner S-cone bipolar cells had primary branches that reached additional S-cone pedicles within our series of sections; for example, iSB3 (red) in color Figures 8 and 9A reached S-cone pedicles #52 and #76. Seven inner S-cone bipolar cells had other primary branches that left the series on the way (we assume) to contact additional S-cone pedicles outside the series (Figs. 8, 10). The pattern of identified S cones in the series was regular, as has been shown to be the case for macaque (Shapiro et al., 1985), and these imagined S cones appeared also to fit in a regular pattern.

Three inner S-cone bipolar cells had their axon terminals within our series. In accordance with other reports (Mariani et al., 1984; Kouyama and Marshak, 1992, 1997; Wässle et al., 1994; Calkins et al., 1998), the terminals stratified in the innermost sublayer of the inner half of the IPL. Two of these three had complete axon terminals. They were reconstructed and described by Calkins et al. (1998), as shown in their Figure 7A. These terminals contacted small bistratified ganglion cells.

For comparison, we tracked and identified the dendritic trees of eight inner midget bipolar cells, each contacted by a single L or M cone. Each inner midget bipolar cell had a single main dendrite emerging from its cell body. As described above, the main dendrite snaked through the inner nuclear layer, remained a single stalk until it neared its cone pedicle, and then broke into a bouquet of smaller branches (Fig. 1C). These branches, which provided central elements to the cone pedicle, almost never ended blindly. Almost every foveal inner midget bipolar cell was contacted by a single L- or M-cone pedicle, with rare inner midget bipolar cells providing a small number of central elements to a neighboring cone pedicle. The terminals of inner midget bipolar cells were also located in the inner

Fig. 4. Serial sections containing two synaptic ribbons, each associated with several central elements, in S-cone pedicle #52. **A–H:** The ribbon at right in this series of electron micrographs has one active zone (R) and four central elements: Central elements 3 (B,C), 7 (C–H), and 8 (H) are provided by one inner S-cone bipolar cell, and central element 4 (C–F) is provided by another. The arciform density structure of the ribbon at left has a gap (B,C), creating two separate arciform densities and two active zones, L1 and L2, each with its own pair of apposed lateral elements. It is therefore called a *double ribbon.* The L1 active zone has three central elements, 1, 5, and 6, obviously arranged in single file, as is evident in the sections shown in D and E. The L2 active zone has three central elements as well, 2, 6, and 7. Central element 6 is shared by active zones L1 and L2, and central element 7 is shared by active zones L2 and R. [Figure 6 shows a reconstruction of ribbon R and a part of ribbon L2 and central elements 3, 4, and 7 in stereo. In the hybrid surface shown in stereo in Figure 9B, the ribbon L (with two active zones) becomes ribbon 9, and the ribbon R becomes ribbon 11.] Scale bar = 1 μm.

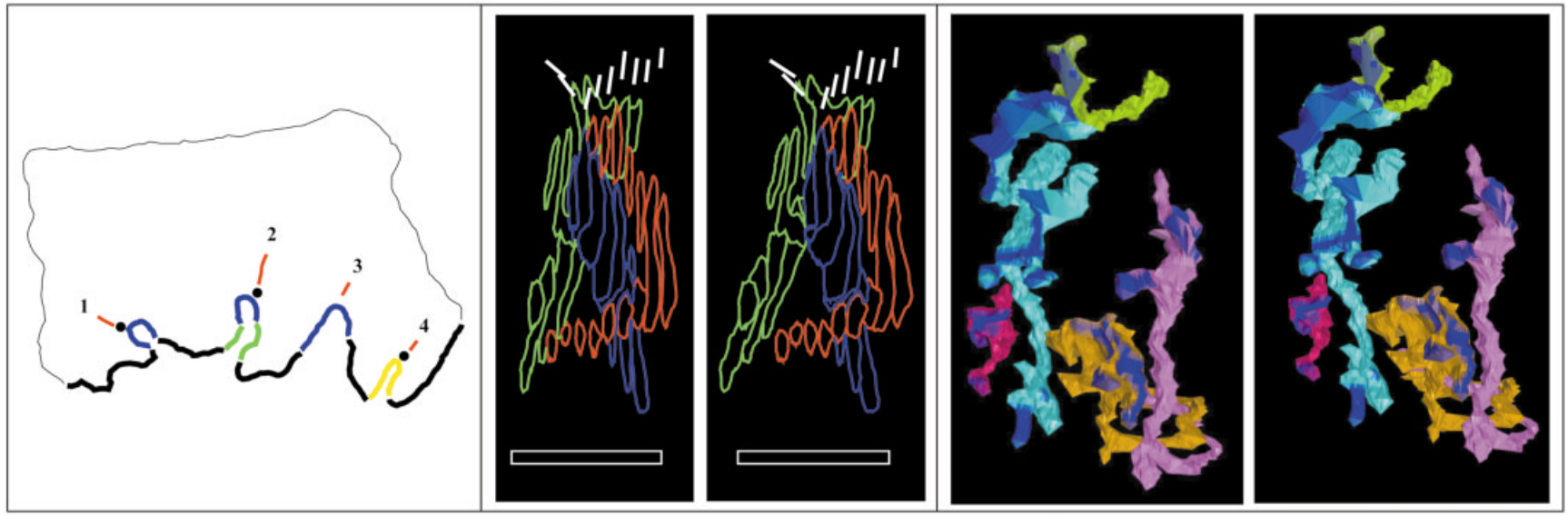

FIG.5 FIG. 6 FIG. 7

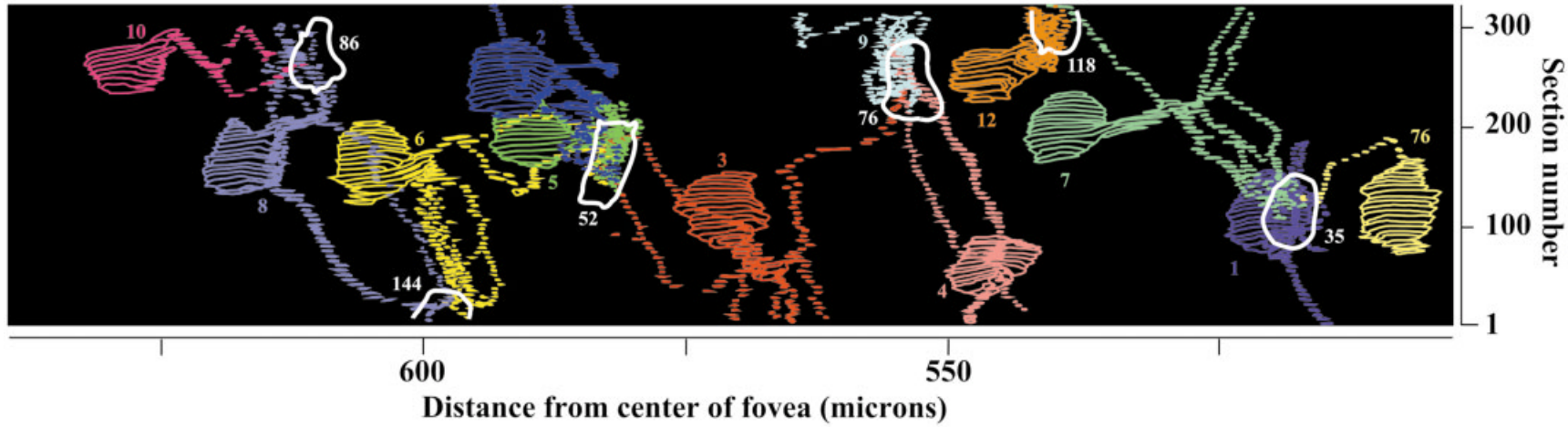

FIG. 8

Figures 5–8.

TABLE 2. Evidence That Particular Bipolar Cells Are Inner S-Cone Bipolar (iSB) Cells

Bipolar ID[1]	Contacted by at least one S cone	Skips non-S cones	Main dendrite branches in innermost OPL	Contacted by multiple S cones in the series	Additional branches that exit the series	Terminal in innermost IPL	Contacts bistratified ganglion cell
iSB1	+	+	+		+	+	+
iSB2	+	+	+		+		
iSB3	+	+	+	+	+	+	+
iSB4	+	+	+		+	+	+
iSB5	+	+	+				
iSB6	+	+	+	+	+		
iSB7	+	+	+	+	+		
iSB8	+	+	+	+	+		
iSB9	+	+	+		+		
iSB10	+	+	+		+		
iSB11	+	+	+		+		
iSB12	+	+	+		+		
iSB dendrites[2]	+	+			+		

[1]In other contexts, iSB1 is also known as bipolar cell 1, iSB2 as 10, iSB3 as 16, iSB4 as 18, iSB5 as 34, iSB6 as 38, iSB7 as 72, iSB8 as 75, iSB9 as 105, iSB10 as 125, iSB11 as 132, and iSB12 as 101.
[2]An *iSB dendrite* was so classified because its primary dendrite skipped non-S cones, but its main dendrite was not in the series. All of these were aggregated as one *cell*, such as iSB4 or iSB8.

(ON) half of the IPL but not as close to the ganglion cell layer as were the terminals of inner S-cone bipolar cells.

S cones contacted an average of four inner S-cone bipolar cells, each of which received input from an average of two S cones

Each inner S-cone bipolar cell provided some but not all of the central elements to a particular S cone. For example, as described above, iSB2 sent five of its seven primary branches to S-cone pedicle #52. The five resulting bundles of dendrites provided 11 central elements (shown as blue tips in Fig. 7) among a total of 43 central elements for pedicle #52 (Table 3A). Thus, iSB2 was responsible for just 26% of all the central elements associated with S-cone pedicle #52.

Several other inner S-cone bipolar cells provided the remaining central elements for S-cone pedicle #52, which is identified by number in Figure 8 and shown by two white outlines at left in Figure 9A. To visualize more clearly the contacts made by S-cone pedicle #52 with its central elements, we created the *hybrid surface* (Schein et al., 1996) shown in color Figure 9B from hybrid contours like the one shown in Figure 5. Hybrid contours consist of the cone pedicle surface, except in regions where the pedicle surface is pushed deeply inward by lateral elements provided by horizontal cells. In those regions, the hybrid surface leaves the pedicle surface and tracks over the central element instead. Chains of gray spheres represent arciform density structures and thus mark the active zones of synaptic ribbons—usually one per synaptic ribbon, but sometimes two. In Figure 9B the ribbons/active zones are numbered from 1 to 23, but ribbons 9 and 12 are double ribbons with two active zones each. Gray regions correspond to the presynaptic membrane of the cone pedicle, excluding the membrane over lateral elements. Blue, green, yellow, red, and pink regions of the hybrid surface are apposed to central elements provided by five inner S-cone bipolar cells, which are color coded as in Figures 8 and 9A. For example, the 11 blue regions of the hybrid

Fig. 5. Color-coded diagram of the cross section of S-cone pedicle #76 shown in Figure 1A. The *hybrid contour* (thick lines) is composed primarily of the basal surface membrane of the pedicle (black). It is called *hybrid* because the part of the pedicle membrane over invaginating lateral elements is omitted and is replaced by the region of apposition between the invaginating tip of the central element and the lateral elements. These regions of the contour and the adjacent regions of apposition between the central element and the cone pedicle are colored (blue, green, and yellow) to represent different inner S-cone bipolar cells. The hybrid contour is bounded by the Müller cell contacts on the left and right (Burris et al., 2002), so the sides and top of the pedicle (thin lines) are not part of the hybrid contour. The synaptic ribbons are red line segments; the arciform densities are marked with circles. (The arciform density of ribbon 3 is absent because it ended prior to this section.)

Fig. 6. Stereo reconstruction showing multiple central elements. Viewers should cross their eyes to see the figure in depth. The reconstruction shows three central elements (from front to back, 3 in blue, 4 in red, and 7 in green) of the four that are postsynaptic to the ribbon R from Figure 4. The ribbon R is shown by the series of seven white line segments on the right. (Central element 8 is small and appears in only one section, so it is omitted here.) Central element 7 is also postsynaptic to the L2 active zone of the double ribbon on the left in Figure 4, so it is *shared.* Part of the L2 ribbon is shown by the series of two white line segments on the left. The central elements line up in single file under ribbon R. (In the hybrid surface shown in stereo in Figure 9B, the ribbon R becomes ribbon 11.) Scale bar = 1 μm.

Fig. 7. Stereo reconstruction of five primary branches of iSB2's dendritic tree invaginating S-cone pedicle #52. Viewers should cross their eyes to see the figure in depth. The reconstruction is oriented as if the viewer were perched on the pedicle, looking toward the bipolar dendrites. Each of the primary branches is colored differently, but all of their central elements are colored blue. The light green branch on the left provides five central elements, the violet branch on the right provides two, the pink branch on the left provides two, the gold branch on the bottom provides one, and the lime green branch on the top provides one, giving an average of 2.2 central elements per primary branch.

Fig. 8. Reconstruction of inner S-cone bipolar cells and their contacts with S cones, overlying the map of cone pedicles (cf. Fig. 2). The reconstruction shows inner S-cone bipolar cell somas in various colors (numbered 1–12), dendrites that reach the six S cones outlined in white (#35, #52, #76, #86, #118, and #144), and additional dendrites that leave the series.

surface in Figure 9B are apposed to the 11 central elements contributed by iSB2 (blue in Figs. 8, 9A). These blue regions are thus complementary to the (blue) central elements at the tips of the dendrites of iSB2 shown in Figure 7.

The five inner S-cone bipolar cells provided 16 (green), 11 (blue), 8 (yellow), 6 (red), and 2 (pink) central elements, or 37%, 26%, 19%, 14%, and 5% of the pedicle's 43 central elements (Table 3A). As was the case with all of the S-cone

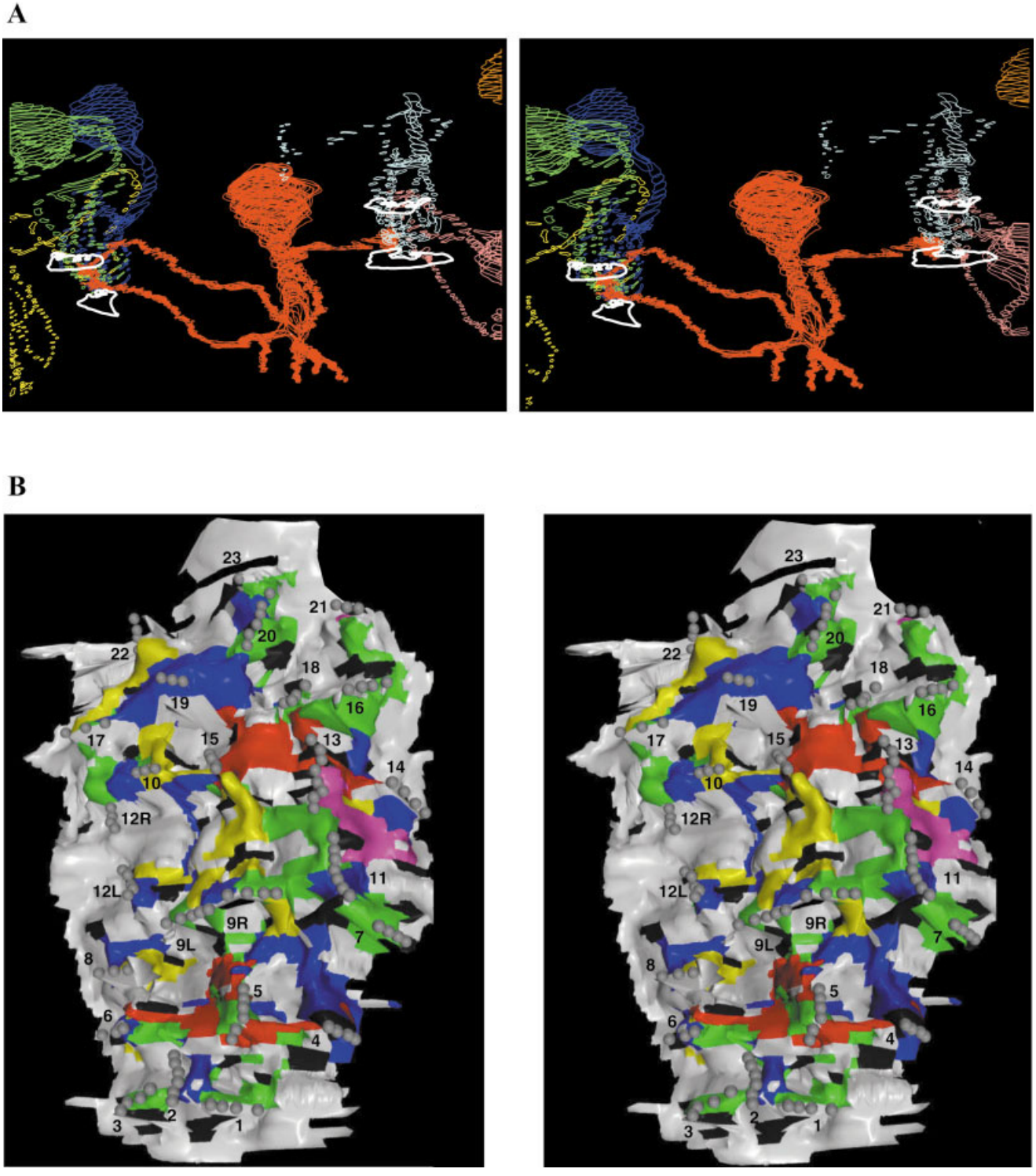

Figure 9

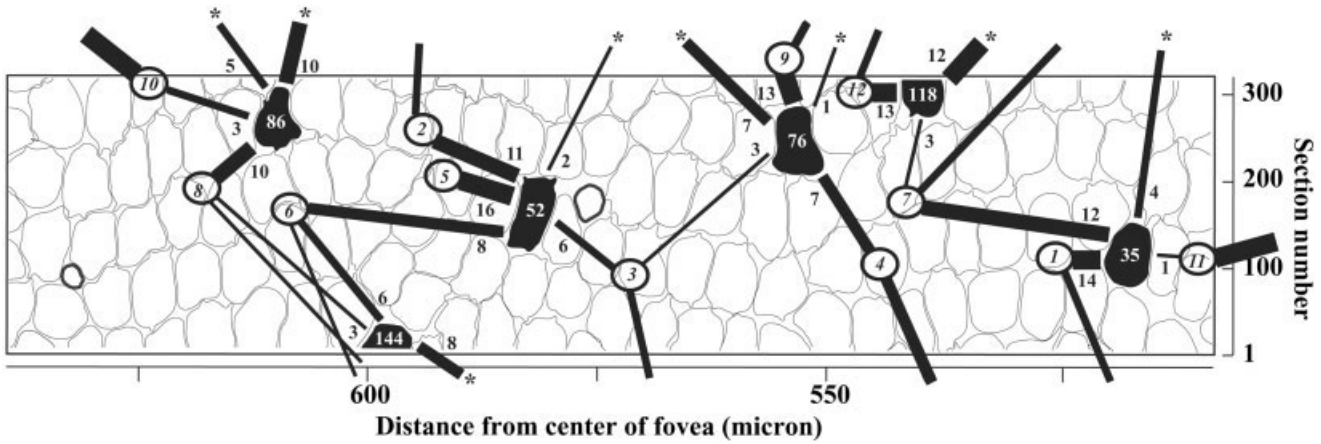

Fig. 10. Schematic map of the 12 inner S-cone bipolar cells. Overlying the map of photoreceptor terminals from Figure 2, this map shows the locations of the inner S-cone bipolar cell somas (1–12), the spread of their dendrites within the series and out of the boundaries of the series, and the S cones to which they provide central elements. In this figure, a single line represents all of the dendritic branches between a particular inner S-cone bipolar cell and a particular S cone. The numbers associated with these lines indicate the number of central elements provided by that bipolar cell to that S cone, with line thickness proportional to that number. Lines that leave the series to provide an unknown number of central elements to S cones outside the series have no associated number. Conversely, lines marked with an asterisk, which enter the series from inner S-cone bipolar cells with neither soma nor main dendrite inside the series, provide a countable number of central elements, so they do have associated numbers.

pedicles in our material, no inner S-cone bipolar cell provided the majority of central elements or was dominant.

The *divergence* of S cones onto inner S-cone bipolar cells was similar for the other S-cone pedicles. To calculate this divergence, for each S cone we noted, for each of its inner S-cone bipolar cells, whether we had the complete set of central elements. We had 13 of these complete sets, accounting for 108 central elements (Table 3A). For one S cone, then, the mean number of central elements provided by one of its inner S-cone bipolar cells was 108/13 = 8.3. Because each inner S-cone bipolar cell provided an average of 8.3 central elements of an S-cone pedicle's average 33.3 central elements, each S-cone pedicle contacted an average of four (33.3/8.3 = 4.0) inner S-cone bipolar cells. Consistent with this calculation, each complete S cone described in Table 3A actually contacted four or five inner S-cone bipolar cells. The diagram in Figure 10 is in agreement with this calculation.

We also computed the *convergence* of S cones onto inner S-cone bipolar cells from the data in Table 3B. Each inner S-cone bipolar cell had an average of 6.0 primary branches. Each primary branch provided an average of 2.7 central elements. Thus, each inner S-cone bipolar cell provided an average of (2.7 × 6.0 =) 16.2 central elements in all. Because an inner S-cone bipolar cell provided an average of 8.3 central elements to each S-cone pedicle in its dendritic field (Table 3A), an average inner S-cone bipolar cell provided central elements to two (16.2/8.3 = 2.0) S cones. The diagram in Figure 10 is in agreement with this calculation as well.

Inner diffuse bipolar cells provided no central elements to S cones

We identified inner diffuse bipolar cells as diffuse primarily because they were contacted by multiple contiguous cone pedicles. The main dendrite of an inner diffuse bipolar cell branches at different depths of the OPL, and the primary branches extend widely in the lateral direction in the OPL, reaching several cone pedicles. The axon terminal of such a cell stratifies in the inner (ON) half of the IPL.

Fig. 9. Stereo reconstructions of an inner S-cone bipolar cell and the hybrid surface of an S-cone pedicle. **A:** Stereo reconstruction of iSB3 and parts of neighboring inner S-cone bipolar cells, following the color coding of cells from Figure 8. Bipolar cell iSB3 provides central elements to S-cone pedicle #52 on the left and S-cone pedicle #76 on the right and sends additional dendrites that course downward to leave the series. Each S-cone pedicle, represented by a pair of white outlined cross sections near its ends, is presynaptic to several other inner S-cone bipolar cells as well. **B:** Stereo reconstruction of the hybrid surface of S-cone pedicle #52. This surface was created by serial reconstruction of hybrid contours such as the one in Figure 5. All the regions of one color are associated with one inner S-cone bipolar cell, with colors following those in Figures 8 and 9A. Ribbons 9 and 12 are double ribbons, each ribbon with two arciform densities that mark their two active zones, 9L (left) and 9R (right) and 12R (upper) and 12L (lower). Each active zone is presynaptic to a triad with its own pair of lateral elements. *Singlet* active zones numbered 1, 2, 3, 7, 12R, 16, 19, 22, and 23 have just one central element; *doublet* active zones numbered 4, 5, 8, 10, 12L, 13, 14, 15, and 21 have two; *triplet* actives zones numbered 6, 9L, 9R, 17, 18, and 20 have three; and *quadruplet* active zone 11 has four. Except for active zones 11, 18, and 20, the central elements postsynaptic to each *multiplet* active zone are provided by different inner S-cone bipolar cells. Active zones 7 and 11 share a central element, as do active zones 9L and 9R, 11 and 13, 16 and 18, and 17 and 19. The 11 blue areas are presynaptic to the central elements provided by iSB2 and are thus complementary to the (blue) tips of that cell's dendrites that are shown in Figure 7. The green, yellow, and red regions are presynaptic to 16, 8, and 6 central elements provided by iSB5, iSB6, and iSB3, respectively. The violet regions are presynaptic to two central elements provided by two dendrites of an inner S-cone bipolar cell that is not in our series.

TABLE 3A. Number of Central Elements Provided by Each Inner S-Cone Bipolar (iSB) Cell to Each S-Cone Pedicle

Bipolar cell	Ped #35 Complete	Ped #52 Complete	Ped #76 Complete	Ped #86 Complete	Ped #118 Complete	Ped #118 Incomplete	Ped #144 Complete	Ped #144 Incomplete	Central elements
iSB1	14								14
iSB2		11							11
iSB3		6	3						9
iSB4			7						7
iSB5		16							16
iSB6		8						6	14
iSB7	12				3				15
iSB8				10			1	2	13
iSB9			13						13
iSB10				4					4
iSB11	1								1
iSB12						13			13
iSB dendrites[1]	4	2	7	5					18
Unidentified dendrites[1]			1	9	12		8		30
Central elements	31	43	31	28	—[2]	—[2]	—[2]	—[2]	(Mean ± SD 33.3 ± 5.8; n = 4)
Identified central elements	31	43	30	19	3	13	1	8	Total = 148
iSB central elements (CE) in complete sets[3]	27	41	23	14	3				Total = 108[3]
Number of sets of CE[3]	3	4	3	2	1				Total = 13[3]
Number of CE/iSB	9.0	10.3	7.7	7.0	3.0				Mean = 8.3 CE/iSB[3]

[1] An *iSB dendrite* was so classified because its primary dendrite skipped non-S cones, but its main dendrite was not in the series. All of these were aggregated as one *cell* such as iSB4 or iSB8. Similarly, all of the *unidentified* (but presumed at this point to be S-cone bipolar cell) dendrites were aggregated as one *cell*. Under these assumptions, each S cone contacted four or five inner S-cone bipolar cells.
[2] This pedicle was incomplete, so its total number of central elements was not included in the calculation of mean.
[3] For five S cones, we had the complete set of central elements provided by inner S-cone bipolar cells in 13 cases. The total number of central elements in these complete sets was 108. For one S cone, the mean number of central elements provided by one of its inner S-cone bipolar cell was thus 108/13 = 8.3.

TABLE 3B. Mean Number of Central Elements Provided by an Inner S-Cone Bipolar (iSB) Cell Branch

Bipolar cell	Number of central elements (CE)	Number of primary branches	Number of primary branches to S-cones	Complete primary branches to S cones	CE from complete primary branches	CE per complete primary branch
iSB1	14	6	4	4	14	3.5
iSB2	11	7	5	4	11	2.2
iSB3	9	6	4	4	9	2.3
iSB4	7	4	3	3	7	2.3
iSB5	16	6	6	6	16	2.7
iSB6	14	6	4	3	8	2.7
iSB7	15	6	4	4	15	3.8
iSB8	13	6	5	4	11	2.8
iSB9	13	7	5	5	13	2.6
iSB10	4	inc	2	2	4	2.0
iSB11	1	inc	1	1	1	1.0
iSB12	13	inc	2	0	0	
iSB dendrites[1]	18					
Unident dendrites[1]	30					
Total	178	54	45	41	109	
Mean		6.0				2.5 (2.7[2])

[1] An *iSB dendrite* was so classified because its primary dendrite skipped non-S cones, but its main dendrite was not in the series. All of these were aggregated as one *cell*, such as iSB4 or iSB8. Similarly, all of the *unidentified* (but presumed at this point to be inner S-cone bipolar cell) dendrites were aggregated as one *cell*. Under these assumptions, each S cone contacted four or five inner S-cone bipolar cells.
[2] The better mean derives from the total numbers, 109/41 = 2.7, so the expected number of central elements/inner S-cone bipolar cell is 6.0 × 2.7 = 16.2

The S cones in our series had a total of 178 central elements. We tracked 148 of these back to inner S-cone bipolar cells or inner S-cone bipolar cell dendrites (Tables 3A, 4A). We tracked exactly zero central elements back to an inner diffuse bipolar cell or an inner diffuse bipolar cell dendrite. Thus, the identifiable central elements of S cones were provided exclusively by a single type of bipolar cell, the inner S-cone bipolar cell.

Moreover, S-cone pedicles #76, #86, #118, and #144 were near the edges of our series (Fig. 2). As a result, the remaining 30 central elements were provided by dendrites that immediately left our series, without having the opportunity to reveal whether they would skip neighboring non-S-cone pedicles and thus be classified as inner S-cone bipolar cells (Figs. 8, 10). For S-cone pedicles #35 and #52, in the interior of our series, the type of bipolar cell or dendrite providing every central element was identified, and every one was identified as an inner S-cone bipolar cell.

By comparison with the S cones, the eight L- and M-cone pedicles that we studied had 17–20 ribbons, no double ribbons, and 17–24 central elements (Table 1B). From among a total of 157 central elements, 125 were provided by inner midget bipolar cells, and 32 (or 20% of the total) were provided by inner diffuse bipolar cells (Table 4B). On average, we identified 15.6 inner midget central elements and 4.0 inner diffuse central elements per L- or M-cone pedicle. Thus, in this foveal region of the retina, a large number of central elements was provided by inner diffuse bipolar cells, making it unlikely that the S cones were missing inner diffuse central elements by chance.

Different bipolar cells provided the central elements of multiplet active zones

In S-cone pedicle #52, several overlapping bundles of fine dendrites supplied by several inner S-cone bipolar cells provided 43 central elements to just 25 active zones

TABLE 4A. Number of Central Elements Provided by Each Type of Bipolar Cell to S-Cone Pedicles

Pedicle	Inner S-cone bipolar cell	Inner S-cone dendrites	Inner midget bipolar cell	Inner diffuse bipolar cell	Unidentfied dendrites	Inner S-cone CE/ identified CE	Diffuse CE/ identified CE
#35	27	4	0	0	0	31/31	0/31
#52	41	2	0	0	0	43/43	0/43
#76	23	7	0	0	1	30/30	0/30
#86	14	5	0	0	9	19/19	0/19
#118	16	0	0	0	12	16/16	0/16
#144	9	0	0	0	8	9/9	0/9
Total	130	18	0	0	30	148/148	0/148

TABLE 4B. Number of Central Elements to L- and M-Cone Pedicles Provided by Each Type of Bipolar Cell

Pedicle	Midget bipolar cell	Diffuse bipolar cells	Total CE	Percentage midget	Percentage diffuse
#17	16	3	19	84	16
#18	13	5	18	72	28
#19	16	4	20	80	20
#23	18	5	23	78	22
#25	16	8	24	67	33
#26	16	1	17	94	6
#42	14	3	17	82	18
#46	16	3	19	84	16
Total	125	32	157	80	20
Mean	15.6	4.0	19.6		

(Table 1A). Among the 43 central elements, 38 (88%) occupied an active zone of a synaptic ribbon with a total of two, three, or four central elements. The situation with the other S-cone pedicles was similar, although only 58% of the central elements of pedicle #35 co-occupied its active zone with another central element.

Remarkably, the central elements occupying the same active zone were almost always supplied by *different* inner S-cone bipolar cells, as can be appreciated from the differently colored central elements associated with each active zone in the hybrid surface of S-cone pedicle #52 (Fig. 9B). In Table 1A, in the columns labeled "doublet," "triplet," and "quadruplet," the numbers in parentheses indicate the number of active zones whose central elements arose from different inner S-cone bipolar cells. In S-cone pedicle #52, for example, the central elements arose from different inner S-cone bipolar cells in nine of nine doublets, in four of six triplets, and in zero of one quadruplet. (In one of the two exceptional triplets and in the exceptional quadruplet, one of the two central elements from the same bipolar cell was shared with another active zone. If the shared central element in each case were to be "assigned" to the other active zone, then those two exceptions would follow the rule, leaving just one exceptional triplet.) Among 52 multiplet active zones in the S cones, 43 (83%) followed the rule that the central elements must be provided by different inner S-cone bipolar cells, and 46 (88%) followed the rule if shared central elements were reassigned.

Eight L and M cones had 26 multiplet ribbons, each with just one active zone (Table 1B). If inner midget (M) bipolar cells supplied 80% of the central elements and inner diffuse (D) bipolar cells provided 20% of the central elements (Table 4B), a random distribution of central elements among the 26 multiplet ribbons would have given 16.6 MM, 8.3 MD, and 1.0 DD combinations. The results were 7 MM, 17 MD, and 2 DD, with DD combinations arising from different inner diffuse bipolar cells. There thus appeared to be a bias in L and M cones, similar to that in S cones, against having an active zone presynaptic to two central elements from the same bipolar cell.

DISCUSSION

This paper reports several new findings on foveal S cones. First, each of these cones has more ribbons, double ribbons, and active zones with multiple central elements than an L or M cone has. Therefore, S cones are presynaptic to more central elements (mean = 33.3) than other cones (mean = 19.6). Second, two types of bipolar cell provide the central elements to L/M cones, with an inner midget bipolar cell providing the most (80%) but with several inner diffuse bipolar cells providing a substantial fraction (20%). By contrast, all the central elements of an S-cone pedicle are provided by just one type of bipolar cell, the inner S-cone bipolar cell. [Nonetheless, because inner diffuse bipolar cells are postsynaptic to cone pedicles at basal contacts as well as at central elements (Calkins et al., 1996; Herr et al., 1996), it is still possible that S cones are presynaptic to inner diffuse bipolar cells.] Third, each S cone is presynaptic to the central elements of four or five inner S-cone bipolar cells.

This paper also reports new findings on foveal inner S-cone bipolar cells. This bipolar cell's main dendrite has an average of 6.0 primary branches, and each branch provides about three (mean = 2.7) central elements to one S cone, so the cell provides an average total of 16.2 central elements. Because it provides an average of 8.3 central elements to *each* S-cone, the average inner S-cone bipolar cell receives convergent ribbon synaptic input from two (16.2/8.3 = 2.0) S cones.

Diversity of active zones in S-cone pedicles

In cone pedicles, the classic picture of an active zone consists of a ribbon that is presynaptic to a triad of invaginating elements: two lateral elements provided by horizontal cell dendrites and a central element provided by an invaginating bipolar cell dendrite (Sjöstrand, 1958; Missotten, 1962, 1965; Dowling and Boycott, 1966; Stell, 1967; Boycott and Dowling, 1969). We observed many variations on this theme in our study; indeed, in some S-cone pedicles, *classic* active zones were in the minority. The most common variation of an active zone involved a ribbon that was presynaptic to multiple central elements, which we call a *multiplet active zone.* Multiplet active zones have been reported previously for all cone types (Boycott and Hopkins, 1991; Kouyama and Marshak, 1992; Chun et al., 1996). Active zones in foveal S cones can have as many as four central elements, as shown in the series of micro-

graphs shown in Figure 4 and illustrated by the stereo reconstruction shown in Figure 6. These central elements line up in single file along the length of the arciform density at the base of the synaptic ribbon, so in cross section the multiplet active zone has the classic triad appearance. The same is true for rod terminals (*spherules*), where what we have termed a *ribbon synaptic unit* contains all or part of one ribbon, one arciform density, one active zone, a pair of apposed lateral elements, and one or more central elements (Migdale et al., 2003).

S-cone pedicles in our series also show *double ribbons,* ribbons with two active zones. [See ribbons 9 and 12 in the hybrid surface of pedicle #52 (Fig. 9B); see also the left (L) ribbon in Fig. 4, which is ribbon 9 of pedicle #52.] Each active zone has a typical organization of two lateral elements and one or more central elements, and the active zones are kept separate by a short *gap,* where the ribbon moves away from the presynaptic membrane. We found ribbons with a maximum of two active zones, but Ahnelt et al. (1990) have observed triple as well as double ribbons. In our sample, we found double ribbons in every complete S-cone pedicle: Three of the pedicles had two double ribbons, and the fourth had one. In contrast, we found a double ribbon in only one of the 19 L- and M-cone pedicles we investigated for this purpose. Curiously, double ribbons are common in rod synaptic terminals (Midgale et al., 2003).

We also found individual central elements that are postsynaptic to two and even three synaptic ribbons. Such a *shared central element* typically reaches between two ribbons or between a double ribbon's two active zones. Kouyama and Marshak (1992) also described central elements shared by two as well as three ribbons. In counting the total number of central elements (Table 1A,B), we were careful not to double-count the shared central elements. Our data (Table 1A,B) therefore suggest that the difference in synaptic organization includes a larger number of ribbons, double ribbons, and multiplets in S cones compared with L and M cones, making each S cone presynaptic to a much larger number of central elements than an L or M cone, 33 vs. 20.

Morphology of inner S-cone bipolar cells

In some respects, our findings regarding inner S-cone bipolar cells are in accordance with previous investigations (Mariani, 1984; Kouyama and Marshak, 1992, 1997; Wässle et al., 1994; Calkins et al., 1998): Many inner S-cone bipolar cells are contacted by more than one S cone, and their dendrites avoid L and M cones. Their main dendrites branch laterally upon reaching the inner region of the OPL. Their fine dendrites reach S cones and provide central elements to triads. Their axon terminals stratify in the innermost region of the IPL.

In other respects, our findings are somewhat different from what has been reported. Kouyama and Marshak (1992) reported that only a *minority* of the central elements invaginating the S cone was stained by their antibody to inner S-cone bipolar cells, an antibody directed against glycine-extended cholecystokinin (CCK), raising the possibility that *most* of the central elements invaginating the S cones were supplied by bipolar cells other than inner S-cone bipolar cells. They also found that most inner S-cone bipolar cells were contacted by *one* S-cone pedicle. These investigators pointed out that both of these observations might have resulted from understaining. We agree. Among the 12 inner S-cone bipolar cells that we identified in our material, 11 were contacted by one or more S-cone pedicles and had branches that extended outside the series, where they were presumably contacted by additional S-cone pedicles (Table 2, Figs. 8, 10). Moreover, we found that every central element that we could classify was provided by an inner S-cone bipolar cell, leaving no central elements for inner diffuse bipolar cells.

Nonredundancy of the source of central elements to ribbons

Multiplet active zones occur frequently, but more so in S-cone pedicles than in L- and M-cone pedicles. Close examination of the central elements in these multiplet active zones reveals that there is a strong tendency for the central elements occupying the same active zone to arise from different bipolar cells (for details see legend to Fig. 9B). Both the S cone's and the L and M cone's invaginating bipolar cells follow this *rule of nonredundancy* in multiplet active zones: In our four complete S cones, the central elements in 36 of the 44 multiplet active zones were provided by different inner S-cone bipolar cells. Similarly, in eight L and M cones, the central elements in 19 of 26 multiplet active zones were provided by different bipolar cells, either one midget and one diffuse or two different diffuse. This bias toward nonredundancy gives these bipolar cells the opportunity to be postsynaptic to as many different active zones as possible.

Comparison of inner S-cone bipolar cells with inner midget bipolar cells

An inner midget bipolar cell provides an average of 15.6 central elements to its single cone, a majority of the average total of 19.6 central elements. Similarly, the inner S-cone bipolar cell is postsynaptic to a single type of cone, and inner S-cone bipolar cells are the main—indeed, the only—source of central elements for S cones. Remarkably, even though an inner S-cone bipolar cell provides central elements to several S cones, it provides an average total of just 16.2, essentially the same number of central elements as provided by a foveal inner midget bipolar cell to an L or M cone. *By this measure, the strength of signal from their separate cones to an inner S-cone bipolar cell and an inner midget bipolar cell appears to be identical.*

Relative numbers of S cones, inner S-cone bipolar cells, and small bistratified ganglion cells

The data in Table 3 allow us to calculate that the signal from one S cone diverges onto an average of four (4.0) inner S-cone bipolar cells, whereas signals from an average of two (2.0) S cones converge onto each inner S-cone bipolar cell, as diagrammed in Figure 3A. In more detail, each S-cone pedicle is presynaptic to an average of 33.3 central elements, but each inner S-cone bipolar cell provides an average of 16.2 central elements. Following Freed et al. (1987) and Sterling et al. (1988), we can use both of these divergence/convergence ratios, 4.0/2.0 and 33.3/16.2, to suggest that inner S-cone bipolar cells must outnumber S cones by almost exactly two to one. Indeed, we found 12 inner S-cone bipolar cell somas in a region that contained six S cones.

By contrast, Kouyama and Marshak (1992) and Wässle et al. (1994) reported that each S cone contacted an average of only 1.8 and 2.4 inner S-cone bipolar cells, respectively. These groups of investigators also reported that each inner S-cone bipolar cell was contacted by an average of only 1.2 and 1.6 S-cone pedicles, respectively. As we mentioned above, both of those studies employed anti-CCK antibodies and may have suffered from incomplete labeling. Indeed, also as noted above, Kouyama and Marshak (1992) labeled the central processes of only eight of 30 active zones in one S-cone pedicle, whereas the results here suggest that they should have labeled all of them.

As described above, these authors' divergence and convergence values could be used to predict the relative numbers of inner S-cone bipolar cells and S cones. Their values give ratios of 1.8/1.2 = 1.5 and 2.4/1.6 = 1.5, which agree with our finding that inner S-cone bipolar cells outnumber S cones, although our 2:1 ratio is greater. In a more recent study of six regions of macaque retina from 5.5 mm to 8.8 mm distance from fovea, however, Kouyama and Marshak (1997) reported a density ratio of inner S-cone bipolar cells to S cones of 1.93 ± 0.35 (mean ± SD). Moreover, Kouyama and Marshak (1992) wrote that the ratio of inner S-cone bipolar cells to S cones does not vary from 60° of visual angle to the fovea.

Several lines of evidence suggest that the number of small bistratified ganglion cells and inner S-cone bipolar cells are equal. First, Calkins et al. (1998) investigated a 2,300 μm^2 region of the IPL (their Fig. 2B), 80 μm (from 560 to 640 μm nasal to the foveal center) × 28.6 μm (319 sections × 0.09 μm/section), and identified six small bistratified ganglion cells. We identified six S cones and 12 inner S-cone bipolar cells in a region of the same tissue that included the region that Calkins et al. (1998) studied but was twice as large, 4600 μm^2, from 480 to 640 μm, a region that ought to have twice as many (hence, 12) small bistratified ganglion cells as Calkins et al. (1998) reported.

Second, in Figure 2B of Calkins et al. (1998), each inner S-cone bipolar cell terminal contacts two to three small bistratified ganglion cells, and, conversely, each ganglion cell receives input from two to three inner S-cone bipolar cells. With divergence (from each inner S-cone bipolar cell onto ~2.5 small bistratified ganglion cells) equal to convergence (of ~2.5 inner S-cone bipolar cells onto each small bistratified ganglion cell), there should be equal numbers of inner S-cone bipolar cells and small bistratified ganglion cells.

Third, each inner S-cone bipolar cell's axon terminal provides an average of 42 ribbon synapses onto its small bistratified ganglion cells, whereas each small bistratified ganglion cell receives an average of 33 contacts from those bipolar cell terminals (Calkins et al., 1998). To accommodate the larger number of bipolar outputs, there would have to be 42/33 = 1.27 ganglion cells for each inner S-cone bipolar cell, consistent with not less but slightly *more* small bistratified ganglion cells than inner S-cone bipolar cells.

These three lines of evidence suggest that the relative numbers of small bistratified ganglion cells, inner S-cone bipolar cells, and S cones are 2:2:1 in the fovea, as captured by the arrangement of cells represented in Figure 3A. In the connectivity diagram in Figure 3B, each S cone is presynaptic to central elements provided by four inner S-cone bipolar cells; in turn, each inner S-cone bipolar cell is postsynaptic to two S cones.

The connections between inner S-cone bipolar cells and small bistratified ganglion cells follow those of Calkins et al. (1998), who reported that nearly all of the ribbon synapses onto a small bistratified ganglion cell converged from two inner S-cone bipolar cells. Therefore, each small bistratified ganglion cell represented in Figure 3B is postsynaptic to two inner S-cone bipolar cells.

With the same numbers of small bistratified ganglion cells and inner S-cone bipolar cells, the divergence of inner S-cone bipolar cells onto small bistratified ganglion cells must be the same as the convergence, so each inner S-cone bipolar cell represented in Figure 3B is presynaptic to two small bistratified ganglion cells. With connectivity as shown in Figure 3B, it follows that small bistratified ganglion cells collect signals from three (or more) S cones in the fovea.

Psychophysics and physiology

Metha and Lennie (2001) suggested, based on psychophysical measurements in human of grating acuity for stimuli that selectively activate S cones and models to account for that data, that a single S cone provides between 80% and 100% of the input to an S-cone ganglion cell at 1° of eccentricity (their Fig. 10). Their model, however, did not take into account the finding presented here that there are twice as many small bistratified ganglion cells as S cones or for the presence of outer S-cone midget ganglion cells. [Every foveal S cone in our series contacts its own outer midget bipolar cell (Klug et al., 1992), which contacts its own outer midget ganglion cell (Klug et al., 1993).] Moreover, our data, summarized in Figure 3, and electrophysiological recordings (Chichilinsky and Baylor, 1999) demonstrate that small bistratified ganglion cells receive substantial input from more than one S cone. Therefore, insofar as their conclusion stands, outer S-cone midget ganglion cells may be the cell responsible for the foveal grating acuity measured by Metha and Lennie (2001) instead of cells in an S-cone ON pathway.

Corresponding psychophysical measurements, functional imaging, and electrophysiologic study show that S cones contribute along with L and M cones to the processing of motion in the dorsal pathway centered on extrastriate visual area MT (Dougherty et al., 1999; Seidemann et al., 1999; Wandell et al., 1999). Is our evidence that foveal S cones do not contact central processes of inner diffuse bipolar cells in conflict with these reports? Study of the diffuse bipolar cells contacted by S cones will be required to resolve this issue. At this time, our evidence does not rule out the possibility that S cones drive outer diffuse bipolar cells or, for that matter, inner diffuse bipolar cells, insofar as inner diffuse bipolar cells receive input from cones at basal contacts as well as at central processes (Calkins et al., 1996).

The *blue-ON* and *yellow-OFF* regions of a small bistratified ganglion cell's receptive field are coextensive (Wiesel and Hubel, 1966; de Monasterio et al., 1975; Derrington and Lennie, 1984; Dacey and Lee, 1994). Calkins et al. (1998) suggested that the yellow-OFF component might be conveyed exclusively by excitatory signals from outer diffuse bipolar cells to bistratified ganglion cells. From study of the same foveal patch that we report here, Calkins et al. estimated that the yellow-OFF receptive field generated by outer diffuse bipolar cells was activated by ~20 L/M cones. In this patch of retina, there are that many (~20) L/M cones for each S cone (Fig. 2). Because of axial chro-

matic aberration, the image of a tiny spot of short-wavelength light is spread over a *blur circle* at the retina with a diameter similar to the spacing between S cones (Marimont and Wandell, 1993; Wandell, 1995; Curcio et al., 1991). Thus, the diameter of the yellow-OFF component provided by outer diffuse bipolar cells to the yellow-OFF receptive field of a small bistratified ganglion cell is no larger than the receptive field of one S cone.

We show, however, that these small bistratified ganglion cells receive substantial input from three or more S cones (Fig. 3B). Thus, for the yellow-OFF receptive field to be coextensive with the blue-ON receptive field, yellow-OFF signals are likely to be conveyed primarily by H2 horizontal cell feedback from L/M cones onto S cones (Ahnelt and Kolb, 1994a,b; Dacey et al., 1996; Goodchild et al., 1996). This conclusion is supported by the paucity of outer bipolar input to the small bistratified ganglion cells in peripheral retina (Ghosh et al., 1997). This conclusion is also supported by Dacey (2000), who reported that blockade of the inner S-cone bipolar (ON) input to small bistratified ganglion cells by 2-amino-4-phosphonobutyric acid (Slaughter and Miller, 1981; Schiller et al., 1986) blocked much of the yellow-OFF signal as well as all of the blue-ON signal.

The experience of color

The experience of color may be described in terms of opponent pairs, blueness-yellowness and redness-greenness (Hering, 1878, 1920; Judd, 1949; Hurvich and Jameson, 1957). Redness has both a long-wavelength and a short-wavelength component, the latter provided by signals from S cones (Werner and Wooten, 1979). The corresponding (+L –M +S) channel has not been found in the retina (de Monasterio and Gouras, 1975) or lateral geniculate nucleus (Derrington et al., 1984; DeValois and DeValois, 1993). Therefore, S-cone signals appear to be added into redness in visual cortex, conveyed by signals from both the S-cone inner (ON) pathway that we address here and the S-cone outer (OFF) midget pathway described by Klug et al. (1993; see also Shinomori et al., 1999). Thus, the perceptual experience generated by activity in these two pathways is violet, not blue, and selective adaptation of these (retinal) pathways follows a tritanopic confusion line in color space rather than a (perceptual) unique blue/unique yellow axis (Krauskopf et al., 1982). Notwithstanding the philosophical obstacles to linking cellular activity with color perception (Valberg, 2001) and the further processing of color in visual cortex, the experience of unique blue appears to require activity in S cones conveyed by these *violet* pathways (with $S > L + M$) and activity in M cones conveyed by L/M opponent (midget) ganglion cells (with $M > L$) to null S-cone redness.

ACKNOWLEDGMENTS

We thank Jim Gayed and Jack Ribble for helping to develop the hybrid pedicle surface (Fig. 9B); Vanessa Preciado for completion of Figures 7 and 9B; Dr. Yoshihiko Tsukamoto, Patricia Masarachia, and Sally Shrom for preparing the EM material; and Kazuki Uema and Lisa Travis for printing. We thank Ivy Ngo for assisting with the article and with Figures 8 and 9A.

LITERATURE CITED

Ahnelt P, Kolb H. 1994a. Horizontal cells and cone photoreceptors in primate retina: a Golgi-light microscopic study of spectral connectivity. J Comp Neurol 343:387–405.

Ahnelt P, Kolb H. 1994b. Horizontal cells and cone photoreceptors in human retina: a Golgi-electron microscopic study of spectral connectivity. J Comp Neurol 343:406–427.

Ahnelt P, Keri C, Kolb H. 1990. Identification of pedicles of putative blue sensitive cones in the human retina. J Comp Neurol 293:39–53.

Boycott BB, Dowling JE. 1969. Organization of the primate retina: light microscopy. Philos Trans R Soc Lond B Biol Sci 255:109–194.

Boycott BB, Hopkins JM. 1991. Cone bipolar cells and cone synapses in the primate retina. Vis Neurosci 7:49–60.

Burris C, Klug K, Ngo IT, Sterling P, Schein S. 2002. How Müller cells in macaque fovea coat and isolate the synaptic terminals of cone photoreceptors. J Comp Neurol 453:100–111.

Calkins DJ, Schein SJ, Tsukamoto Y, Sterling P. 1994. M and L cones in macaque fovea connect to midget ganglion cells by different numbers of excitatory synapses. Nature 371:70–72.

Calkins D, Tsukamoto Y, Sterling P. 1996. Foveal cones form basal as well as invaginating junctions with diffuse ON bipolar cells. Vis Res 36: 3373–3381.

Calkins D, Tsukamoto Y, Sterling P. 1998. Microcircuitry and mosaic of a blue-yellow ganglion cell in the primate retina. J Neurosci 18:3373–3385.

Chichilinsky EJ, Baylor DA. 1999. Receptive-field microstructure of blue-yellow ganglion cells in primate retina. Nat Neurosci 2:889–893.

Chun M, Grünert U, Martin P, Wässle H. 1996. The synaptic complex of cones in the fovea and in the periphery of the macaque monkey retina. Vis Res 36:3383–3395.

Cottaris N, DeValois R. 1998. Temporal dynamics of chromatic tuning in macaque primary visual cortex. Nature 395:896–900.

Curcio CA, Allen KA, Sloan KR, Lerea CL, Hurley JB, Klock IB, Milam AB. 1991. Distribution and morphology of human cone photoreceptors stained with anti-blue opsin. J Comp Neurol 312:610–624.

Dacey DM. 1993a. The mosaic of midget ganglion cells in the human retina. J Neurosci 13:5334–5355.

Dacey DM. 1993b. Morphology of a small-field bistratified ganglion cell type in the macaque and human retina. Vis Neurosci 10:1081–1098.

Dacey DM. 1996. Circuitry for color coding in the primate retina. Proc Natl Acad Sci USA 93:582–588.

Dacey DM. 2000. Parallel pathways for spectral coding in primate retina. Annu Rev Neurosci 23:743–775.

Dacey DM, Lee BB. 1994. The "blue-ON" opponent pathway in primate retina originates from a distinct bistratified ganglion cell type. Nature 367:731–735.

Dacey DM, Lee BB, Stafford DK, Pokorny J, Smith VC. 1996. Horizontal cells of the primate retina: cone specificity without spectral opponency. Science 271:656–659.

de Monasterio FM, Gouras P. 1975. Functional properties of ganglion cells in the rhesus monkey retina. J Physiol (London) 251:167–199.

Derrington AM, Lennie P. 1984. Spatial and and temporal contrast sensitivities of neurones in lateral geniculate nucleus of macaque. J Physiol 357:219–240.

Derrington AM, Krauskopf J, Lennie P. 1984. Chromatic mechanisms in lateral geniculate nucleus of macaque. J Physiol 357:241–265.

DeValois RL, DeValois KK. 1993. A multi-stage color model. Vis Res 33:1053–1065.

Dougherty RF, Press WA, Wandell BA. 1999. Perceived speed of colored stimuli. Neuron 24:893–899.

Dowling JE, Boycott BB. 1966. Organization of the primate retina: electron microscopy. Proc R Soc Lond B Biol Sci 166:80–111.

Esfahani P, Schein SJ, Klug K, Tsukamoto Y, Sterling P. 1993. Characterization of L, M, and S cone pedicles in primate fovea. Soc Neurosci Abstr 19:1201.

Famiglietti EV Jr, Kolb H. 1976. Structural basis for ON-and OFF-center responses in retinal ganglion cells. Science 194:193–195.

Freed MA, Smith RG, Sterling P. 1987. Rod bipolar array in the cat retina: pattern of input from rods and GABA-accumulating amacrine cells. J Comp Neurol 266:445–455.

Ghosh KK, Martin PR, Grünert U. 1997. Morphological analysis of the blue cone pathway in the retina of a new world monkey, the marmoset *Callithrix jacchus*. J Comp Neurol 379:211–225.

Goodchild AK, TL Chan TL, Grünert U. 1996. Horizontal cell connections with short-wavelength cones in macaque monkey retina. Vis Neurosci 13:833–845.

Hering E. 1878. Zur Lehre von Lichtsinne. Vienna: C. Gerold's Sohn.

Hering E. 1920. Outline of a theory of the light sense, trans. Hurvich LM, Jameson D. 1964. Cambridge, MA: Harvard University Press.

Herr SS, Tiv N, Sterling P, Schein SJ. 1996. S cones in macaque fovea are invaginated by one type of ON bipolar cell, but L and M cones are invaginated by midget and diffuse bipolar cells. Invest Ophthalmol Vis Sci Suppl 37:S1059.

Hopkins JM, Boycott BB. 1995. Synapses between cones and diffuse bipolar cells of a primate retina. J Neurocytol 24:680–694.

Hurvich L, Jameson D. 1957. An opponent-process theory of color vision. Psychol Rev 64:384–404.

Judd DV. 1949. Response functions for types of vision according to the Muller theory. J Res Natl Bur Stand 42:1–16.

Klug K, Schein SJ, Masarachia P, Sterling P, Tsukamoto Y. 1991. Identification of all cells in a small patch of fovea of macaque retina. Soc Neurosci Abstr 17:1375.

Klug K, N Tiv N, Y Tsukamoto Y, P Sterling P, Schein SJ. 1992. Blue cones contact Off-midget bipolar cells. Soc Neurosci Abstr 18:838.

Klug K, Tsukamoto Y, P Sterling P, Schein SJ. 1993. Blue cone off-midget ganglion cells in macaque. Invest Ophthalmol Vis Sci Suppl 34:986.

Kolb H. 1970. Organization of the outer plexiform layer of the primate retina: electron microscopy of Golgi-impregnated cells. Philos Trans R Soc Lond B Biol Sci 258:261–283.

Kouyama N, Marshak DW. 1992. Bipolar cells specific for blue cones in the macaque retina. J Neurosci 12:1233–1252.

Kouyama N, Marshak DW. 1997. The topographical relationship between two neuronal mosaics in the short wavelength-sensitive system of the primate retina. Vis Neurosci 14:159–167.

Krauskopf J, Williams DR, Heeley DW. 1982. Cardinal directions of color space. Vis Res 22:1123–1131.

Lennie P, D'Zmura M. 1988. Mechanisms of color vision. Crit Rev Neurobiol 3:333–400.

Mariani AP. 1984. Bipolar cells in monkey retina selective for the cones likely to be blue-sensitive. Nature 308:184–186.

Marimont D, Wandell B. 1993. Matching color images: the effects of axial chromatic aberration. J Opt Soc Am A12:3113–3122.

Metha AB, Lennie P. 2001. Transmission of spatial information in S-cone pathways. Vis Neurosci 18:961–972.

Meyers D, Skinner S, Sloan K. 1992. Surfaces from contours. ACM Trans Graphics 11:228–258.

Migdale K, Herr S, Klug K, Ahmad K, Linberg K, Sterling P, Schein SJ. 2003. Two ribbon synaptic units in rod photoreceptors of macaque, human, and cat. J Comp Neurol 455:100–112.

Missotten L. 1962. L'ultrastructure des cônes de la rétine humaine. Bull Soc Belge Ophtalmol 130:472–502.

Missotten L. 1965. The ultrastructure of the human retina. Brussels: Editons Arscia S.A.

Nelson R, Famiglietti EV Jr, Kolb H. 1978. Intracellular staining reveals different levels of stratification for on- and off-center ganglion cells in cat retina. J Neurophysiol 41:472–483.

Polyak S. 1941. The retina. Chicago: The University of Chicago Press.

Rodieck RW. 1991. Which cells code for color? In: Valberg A, Lee BB, editors. From pigments to perception: advances in understanding visual processes. New York: Plenum Press. p 83–89.

Schein SJ. 1988. Anatomy of macaque fovea and spatial densities of neurons in foveal representation. J Comp Neurol 269:479–505.

Schein SJ, Gayed JM, Herr SS, Sterling P, Klug K. 1996. Cone ribbon synapses might supply basal synapses with glutamate. Invest Ophthalmol Vis Sci Suppl 37:S6.

Schiller PH, Sandell JH, Maunsell JH. 1986. Functions of the ON and OFF channels of the visual system. Nature 322:824–825.

Seidemann E, Poirson AB, Wandell BA, Newsome WT. 1999. Color signals in area MT of the macaque monkey. Neuron 24:911–917.

Shapiro MB, Schein SJ, de Monasterio FM. 1985. Regularity and structure of the spatial pattern of blue cones of macaque retina. J Am Statist Assoc 80:803–814.

Shinomori K, Spillmann L, Werner JS. 1999. S-cone signals to temporal OFF-channels: asymmetrical connections to postreceptoral chromatic mechanisms. Vis Res 39:39–49.

Sjöstrand FS. 1958. Ultrastructure of retinal rods synapses of the guinea pig eye as revealed by three-dimensional reconstructions from serial sections. J Ultrastruct Res 2:122–170.

Slaughter MM, Miller RF. 1981. 2-Amino-4-phosphonobutyric acid: a new pharmacological tool for retina research. Science 211:182–185.

Smith RG. 1987. Montage: a system for three-dimensional reconstruction by personal computer. J Neurosci Methods 21:55–69.

Stell WK. 1967. The structure and relationships of horizontal cells and photoreceptor-bipolar synaptic complexes in goldfish retina. Am J Anat 121:401–424.

Sterling P, Freed MA, Smith RG. 1988. Architecture of rod and cone circuits to the on-beta ganglion cell. J Neurosci 86:23–42.

Tsukamoto Y, Masarachia P, Schein SJ, Sterling P. 1992. Gap junctions between the pedicles of macaque foveal cones. Vis Res 32:1809–1815.

Valberg A. 2000. Unique hues: an old problem for a new generation. Vis Res 41:1645–1657.

Valberg A, Lee BB, Tigwell DA. 1986. Neurones with strong inhibitory S-cone inputs in the macaque lateral geniculate nucleus. Vis Res 26: 1061–1064.

Wandell BA. 1995. Foundations of vision. Sunderland, MA: Sinauer Associates.

Wandell BA, Poirson AB, Newsome WT, Baseler HA, Boynton GM, Huk A, Gandhi S, Sharpe LT. 1999. Color signals in human motion-selective cortex. Neuron 24:901–909.

Wässle H, Grünert U, Martin PR, Boycott BB. 1994. Immunocytochemical characterization and spatial distribution of midget bipolar cells in the macaque monkey retina. Vis Res 34:561–79.

Wiesel TN, Hubel DH. 1966. Spatial and chromatic interactions in the lateral geniculate body of the rhesus monkey. J Neurophysiol 29:1115–1156.

Wooten BR, Werner JS. 1979. Short-wave cone input to the red-green opponent channel. Vis Res 19:1053–1054.